Oxyresveratrol induces apoptosis and inhibits cell viability via inhibition of the STAT3 signaling pathway in Saos-2 cells

TAO LV*, ZHEN JIAN*, DEJIAN LI, RONGGUANG AO, XU ZHANG and BAOQING YU

Department of Orthopedics, Shanghai Pudong Hospital, Fudan University Pudong Medical Center, Shanghai 201399, P.R. China

Received May 30, 2020; Accepted September 17, 2020

DOI: 10.3892/mmr.2020.11591

Abstract. Oxyresveratrol (ORES) is a natural phenolic compound with multiple biological functions including anti-oxidation, anti-inflammation and neuroprotection; however, the inhibitory effect of ORES on osteosarcoma remains largely unknown. The present study aimed to determine the effects of ORES on osteosarcoma cell Saos-2. Cell Counting Kit-8 assay was performed to detect Soas-2 cell viability. Annexin-FITC/PI staining and JC-1 staining were used to measure cell apoptosis and the change of mitochondrial membrane potential. In addition, western blotting was conducted to determine the expression levels of apoptotic proteins and the phosphorylation of STAT3. It was found that ORES inhibited cell viability and induced apoptosis of osteosarcoma Saos-2 cells in a concentration-dependent manner. In addition, ORES increased the expression levels of apoptotic proteases caspase-9 and caspase-3 and reduced mitochondrial membrane potential. In response to ORES treatment, the expression levels of pro-apoptotic proteins, Bad and Bax, were enhanced, whereas those of anti-apoptotic proteins, Bcl-2 and Bcl-xL, were reduced. In addition, the phosphorylation of STAT3 was attenuated in Saos-2 cells after treatment with ORES. Inhibition of cell viability and apoptosis induction by ORES were rescued by enhancement of STAT3 activation upon treatment with IL-6. Collectively, the present study indicated that ORES induced apoptosis and inhibited cell viability, which may be associated with the inhibition of STAT3 activation; thus, ORES represents a promising agent for treating osteosarcoma.

Correspondence to: Professor Baoqing Yu, Department of Orthopedics, Shanghai Pudong Hospital, Fudan University Pudong Medical Center, 2800 Gongwei Road, Pudong, Shanghai 201399, P.R. China
E-mail: doctorybq@126.com

*Contributed equally

Key words: oxyresveratrol, osteosarcoma, viability, apoptosis, STAT3

Introduction

Osteosarcoma is the most common primary malignant bone tumor of mesenchymal origin that occurs primarily in children and adolescents (1). It is characterized by the production of calcified osteoid extracellular matrix and a high frequency of inducing lung metastases, which directly results in a high mortality rate (2). The 5-year survival rate of patients with local osteosarcoma ranges between 65 and 75%, whereas that of patients with metastatic osteosarcoma is <30% (3). Surgical resection, chemotherapy and radical resection are established strategies for treating patients with osteosarcoma (4,5). Immunotherapy or a combination of radiotherapy and immunotherapy using nanomaterial delivery systems have also been a research hotspot in the field (6-8). However, the 5-year survival rate of patients with osteosarcoma demonstrates little improvement after treatment with chemotherapy drugs and traditional amputation (4). Therefore, it is important to identify new effective agents for treating patients with osteosarcoma.

Certain malignant tumors present an anti-apoptotic phenotype, which allows cancer cells to survive in local tissues (9). Most of the current anticancer medicines target apoptotic signaling pathways (10). Activation of caspases can be initiated via both the extrinsic and the mitochondria-mediated apoptotic signaling pathways (10-12). The extrinsic pathway is triggered by activation of caspase-8 at the plasma membrane upon ligation of the death receptor, and subsequent cleavage of downstream effector caspases, such as caspase-3 (10). The mitochondria-mediated signaling pathway relies on interactions among Bcl-2 family proteins at the mitochondrial outer membrane and the release of cytochrome *c* (11). Among Bcl-2 family proteins, the activators directly bind both anti-apoptotic proteins and pro-apoptotic effector proteins, while sensitizers such as Bad bind only anti-apoptotic proteins (11,12). By competing for the BH3 binding site, sensitizers displace the binding of activators to anti-apoptotic proteins, including Bcl-2 and Bcl-xL (11). By interacting with the activators, pro-apoptotic effector proteins such as Bax and Bak create openings in the outer mitochondrial membrane and release cytochrome *c*, which promotes caspase-9 activation, followed by a cascade of apoptotic proteases, including caspase-3, resulting in cell death (12). The increased permeability of the mitochondrial outer membrane also results in mitochondrial depolarization with reduced mitochondrial membrane potential (MMP) and

the release of apoptotic factors, triggering the downstream cell death processes (13-15). Venetoclax, a direct small molecular inhibitor of Bcl-2, was initially approved by the Food and Drug Administration (FDA) in April 2016 and exhibited impressive outcomes particularly in chronic lymphocytic leukemia, small lymphocytic lymphoma and acute myeloid leukemia (16).

STAT3-mediated signaling pathways have an oncogenic potential in cancer cell proliferation and metastasis (17). The expression levels of STAT3 have been reported to be significantly higher in osteosarcoma tissue compared with those in normal bone or cartilage tissue, and high levels of STAT3 are associated with poor tumor differentiation and metastasis (18). Five-year overall survival and relapse-free survival rates in patients with high STAT3 expression levels are lower compared with in those with low STAT3 expression levels (18). Inhibition of STAT3 has also been reported to suppress osteosarcoma cell growth and induce apoptosis (19). Therefore, STAT3 may have an important therapeutic and prognostic value in osteosarcoma. In addition, STAT3 is directly involved in transcriptional regulation of osteopontin (OPN) (20), and increased OPN expression levels serve a critical role in osteosarcoma, which is a potential biomarker and promising drug target for osteosarcoma (21).

As a natural ingredient, which is primarily found in *Morus alba* L., oxyresveratrol (ORES) has extensive biological effects. Over the previous two decades, ORES has been reported as a powerful tyrosinase activity inhibitor (22,23), and also as having antioxidative (24,25), anti-inflammatory (26,27), anticancer (28-30) and anti-lipogenesis properties (31). ORES has also been observed to exert strong neuroprotective effects, as it reduces neuronal oxidative damage (32,33). Notably, ORES and its derivatives have been reported to serve an efficient role against various types of cancer, such as head and neck carcinoma (28), neuroblastoma (29), prostate (30), kidney (34) and lung cancer (35). However, it remains unknown whether ORES has an effect on the inhibition of osteosarcoma cells and the mechanism by which ORES inhibits tumor cell viability.

In the present study, the inhibitory effect of ORES on Saos-2 osteosarcoma cells was determined, which indicates the ORES is a promising agent for treating osteosarcoma.

Materials and methods

Compound and reagents. ORES (2,3',4,5'-Tetrahydroxy-trans-stilbene, $C_{14}H_{12}O_4$; molecular weight: 244.24; purity ≥97.0%; cat. no. 29700-22-9) was purchased from Sigma-Aldrich (Merck KGaA). DMSO was used as control. DMEM, penicillin and streptomycin solution (100 IU/ml; 100 μg/ml), PBS, 0.25% trypsin-EDTA and enhanced chemiluminescent (ECL) substrate were all provided by Thermo Fisher Scientific, Inc. Fetal bovine serum (FBS) was obtained from Hangzhou Sijiqing Biological Engineering Materials Co., Ltd. Cell Counting Kit (CCK)-8 assay kit, MMP assay kit with JC-1, bicinchoninic acid (BCA) protein assay kit and RIPA lysis buffer (cat. no. P0013B) were acquired from Beyotime Institute of Biotechnology. Annexin V-FITC/propidium iodide (PI) apoptosis detection kit was purchased from MultiSciences (Lianke) Biotech Co., Ltd. Tris, non-fat milk and Tween-20 were purchased from Sangon Biotech Co., Ltd. IL-6 was purchased from PeproTech, Inc. Primary antibodies against cleaved caspase-9 (cat. no. 20750), cleaved caspase-3 (cat. no. 9664), GAPDH (cat. no. 5174), Bcl-2 (cat. no. 4223), Bcl-xL (cat. no. 2764), Bad (cat. no. 9239), Bax (cat. no. 5023), phophorylated-STAT3 (P-STAT3; cat. no. 9145) and total-STAT3 (T-STAT3; cat. no. 12640) were obtained from Cell Signaling Technologies, Inc. An antibody against OPN (cat. no. 7C5H12) was obtained from Thermo Fisher Scientific, Inc. Horseradish peroxidase (HRP)-conjugated anti-rabbit antibody (cat. no. 111-035-003) and HRP-conjugated anti-mouse antibody (cat. no. 115-035-003) were supplied by Jackson ImmunoResearch Laboratories, Inc. Methanol and ethanol were obtained from Sinopharm Chemical Reagent Co., Ltd.

Cell culture and cell viability assay. Saos-2 cells were obtained from the American Type Culture Collection. Cells were grown in DMEM containing 10% FBS and 1% penicillin and streptomycin solution with 5% CO_2 at 37˚C. Cell passage was performed with 0.25% trypsin-EDTA.

Cell viability was detected using the CCK-8 assay kit according to the manufacturer's instructions. Briefly, cells were seeded in 12-well plates at a density of $4x10^5$ cells/well. After attachment, the cells were incubated with ORES at 0, 5, 15 and 45 μM at 37˚C for 48 h. The CCK-8 solution (10 μl) was added to each well and after 1.5 h incubation, the viability of Saos-2 cells was detected using a microplate reader at 450 nm. In certain experiments, the Saos-2 cells were incubated with 30 μM ORES or 30 μM ORES and 20 ng/ml IL-6 at 37˚C for 24 h.

Apoptosis assay. Early and late apoptosis was detected using the Annexin V-FITC/PI apoptosis detection kit according to the manufacturer's instructions. Cells were seeded in 12-well plates at a density of $4x10^5$ cells/well. After attachment, the cells were incubated with ORES at 0, 5, 15 and 45 μM at 37˚C for 24 h. The cells were then washed twice with ice-cold PBS. After digestion with 0.25% trypsin-EDTA, cells were collected and washed with PBS. Cells were resuspended in 400 μl Annexin-binding buffer, and then incubated with 5 μl Annexin V-FITC and 10 μl PI at room temperature for 5 min. Apoptosis of Saos-2 cells was detected with a LSRFortessa TM X-20 flow cytometer (BD Biosciences). Given that ORES significantly inhibited Saos-2 cell viability at the concentration between 15 and 45 μM, the Saos-2 cells was incubated with 30 μM ORES or 30 μM ORES and 20 ng/ml IL-6 at 37˚C for 24 h. FlowJo 7.6 software (Tree Star, Inc.) was used for data processing.

MMP measurement. Changes in MMP were detected using the MMP assay kit with JC-1 staining, according to the manufacturer's instructions. Cells were seeded in 12-well plates at a density of $4x10^5$ cells/well. After attachment, cells were incubated with ORES at 0, 5, 15 and 45 μM at 37˚C for 24 h. The cells were then harvested and washed with PBS. After incubation with JC-1 staining solution for 20 min at 37˚C in the dark, cells were washed twice with JC-1 buffer. Finally, cells were resuspended in PBS and detected using a LSRFortessa TM X-20 flow cytometer (BD Biosciences). FlowJo 7.6 software (FlowJo LLC) was used for data processing. The polymer/monomer (red/green) fluorescence intensity ratio was used to quantify the MMP.

Western blotting. Saos-2 cells were seeded in 6-well plates at 1x10^6 cells/well overnight at 37˚C, and were then incubated with ORES at 0, 5, 15 and 45 μM at 37˚C for 24 h. In some experiments, the Saos-2 cells were incubated with 30 μM ORES or 30 μM ORES and 20 ng/ml IL-6 at 37˚C for 24 h. After washing with cold phosphate-buffered saline (PBS) three times, cells were lysed in RIPA lysis buffer and the protein concentration was detected using a BCA protein assay kit, according to the manufacturer's instructions. Each sample was adjusted to the same concentration with lysis buffer and 20 μg protein was loaded per lane. Proteins were then separated by SDS-PAGE on 10% gels and were transferred to 0.45 μm nitrocellulose filter membranes. The membranes were washed and blocked in blocking buffer (5% non-fat milk) for 1 h at room temperature. Subsequently, the membranes were incubated with primary antibodies against cleaved caspase-9, cleaved caspase-3, GAPDH, Bcl-2, Bcl-xL, Bad, Bax, P-STAT3, T-STAT3 and OPN (diluted at 1:1,000) with gentle agitation overnight at 4˚C. After three washes, the membrane was incubated with HRP-conjugated anti-rabbit secondary antibody (diluted at 1:3,000) with gentle agitation for 2 h at room temperature. Finally, the ECL reagent was used to detect the target proteins. Semi-quantification of the bands was performed using ImageJ software (1.48v; National Institutes of Health).

Statistical analysis. The experiments were repeated at least three times independently, and data were presented as the mean ± SEM. One-way ANOVA followed by Tukey's post hoc test was applied to compare the differences between groups, using GraphPad Prism 5 (GraphPad Software, Inc.). *P<0.05 was considered to indicate a statistically significant difference.

Results

ORES inhibits the viability of Saos-2 cells. Although ORES has been shown to inhibit prostate and colon cancer cell viability (30), it remains unknown whether ORES can inhibit osteosarcoma cell viability. As a natural phenolic compound, ORES is a resveratrol analogue that contains an additional hydroxyl group in the aromatic ring (22). The chemical structure of ORES is shown in Fig. 1A. To determine the effect of ORES on the proliferation of osteosarcoma cells, the cell viability following ORES treatment in the Saos-2 cell line was detected. Cells were incubated with ORES at 0, 5, 15 and 45 μM for 48 h, and cell viability was detected using the CCK-8 assay. The results demonstrated that ORES significantly reduced cell viability in a concentration-dependent manner (Fig. 1B). These results indicated that ORES inhibits osteosarcoma cell viability.

ORES induces apoptosis of Saos-2 cells. Although ORES has been reported to induce apoptosis of neuroblastoma cells (29), the effect on osteosarcoma cells remains unclear. Following incubation with ORES at 0, 5, 15 and 45 μM for 24 h, apoptotic cells were detected using Annexin-FITC/PI staining. The results demonstrated that treatment with ORES significantly increased the percentage of apoptotic cells in a concentration-dependent manner compared with that of the untreated group (Fig. 1C and D).

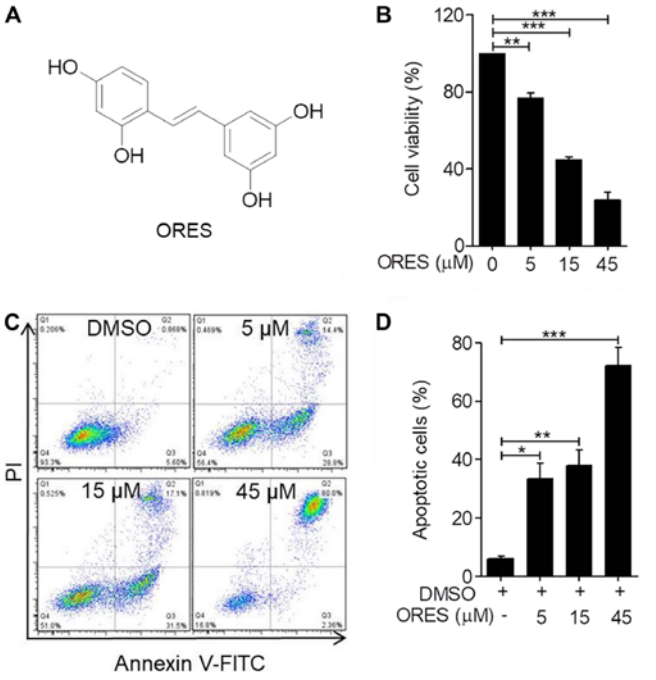

Figure 1. ORES inhibits cell proliferation and induces apoptosis of Saos-2 cells. (A) Chemical structure of ORES. (B) Saos-2 cells were incubated with ORES at 0, 5, 15 and 45 μM for 48 h. Cell viability was detected using the Cell Counting Kit-8 assay. (C) Saos-2 cells were incubated with ORES at 0, 5, 15 and 45 μM for 24 h. Cells were then collected and underwent Annexin-FITC/PI staining. Apoptosis was measured with flow cytometry and Annexin V-FITC positive cells were identified as apoptotic cells. (D) Percentage of Saos-2 apoptotic cells was quantified. The experiments were repeated at least three times and the results are shown as the mean ± SEM. *P<0.05, **P<0.01, ***P<0.001. ORES, oxyresveratrol; PI, propidium iodide.

A decrease in MMP is a marker of early apoptosis. In the mitochondria of normal cells, JC-1 is present as a polymer with bright red fluorescence. Once the mitochondria-mediated apoptotic pathway is initiated, JC-1 cannot aggregate and the JC-1 monomer generates green fluorescence, according to the manufacturer's instructions. The relative ratio of polymer/monomer (red/green) fluorescence was used to measure the mitochondrial depolarization. In response to ORES treatment at 0, 5, 15 and 45 μM for 24 h, cells were clearly divided into two groups, with polymer at the top and monomer at the bottom (Fig. 2A). The ratio of JC-1 polymer/monomer significantly decreased in a concentration-dependent manner in response to ORES compared with that of the untreated group (Fig. 2B).

In the mitochondria-mediated pathway, cytochrome *c* is released from mitochondria and induces the cleavage of caspase-3 and caspase-9, which ultimately triggers apoptosis via proteolysis of several cytoskeletal proteins, as well as the cleavage of DNA via caspase-activated DNase (12). The results of the present study demonstrated that compared with those of the untreated group, the expression levels of cleaved caspase-9 and cleaved caspase-3 were significantly increased by ORES treatment in a concentration-dependent manner (Fig. 3A-C). These results suggested that ORES induces osteosarcoma apoptosis.

ORES modulates apoptotic signaling pathways in Saos-2 cells. Given that ORES was demonstrated to promote apoptosis, the mechanism by which ORES regulates the apoptotic

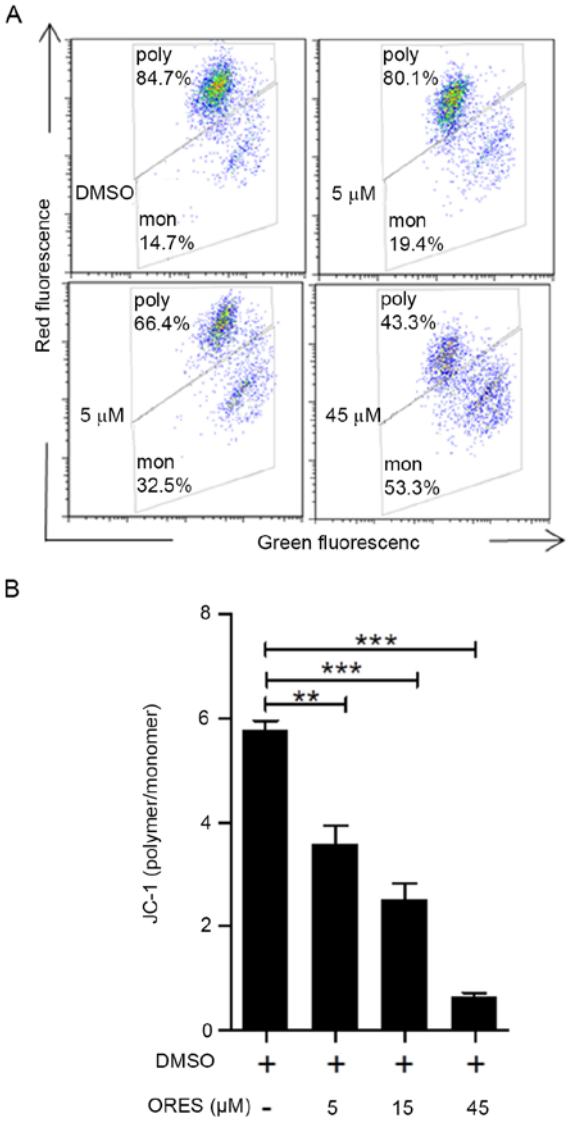

Figure 2. ORES inhibits the MMP of Saos-2 cells. Saos-2 cells were incubated with ORES at 0, 5, 15 and 45 μM for 24 h. The cells were then collected, and were stained with JC-1. (A) Changes in MMP were detected by flow cytometry. (B) Polymer/monomer ratio was calculated and quantified. The experiments were repeated three times and the results are shown as the mean ± SEM. **P<0.01, ***P<0.001. ORES, oxyresveratrol; MMP, mitochondrial membrane potential; mon, monomer; poly, polymer.

signaling pathways was further investigated. Western blotting was used to detect the expression levels of Bcl-2 family proteins, including Bcl-2, Bcl-xL, Bad and Bax (Fig. 4A). Mitochondria-mediated apoptosis is regulated by Bcl-2 family proteins (10). Pro-apoptotic sensitizer protein Bad can bind anti-apoptotic proteins Bcl-2 and Bcl-xL, which cause pro-apoptotic activator proteins to dissociate from these anti-apoptotic proteins and then bind to pro-apoptotic effector proteins, such as Bax, to initiate apoptosis (11). Compared with those of the untreated group, following treatment with ORES the expression levels of anti-apoptotic proteins Bcl-2 (Fig. 4B) and Bcl-xL (Fig. 4C) were significantly decreased, whereas the expression levels of pro-apoptotic proteins Bad (Fig. 4D) and Bax (Fig. 4E) were significantly increased. These results suggested that ORES may regulate the mitochondria-mediated apoptotic signaling pathway in Saos-2 cells.

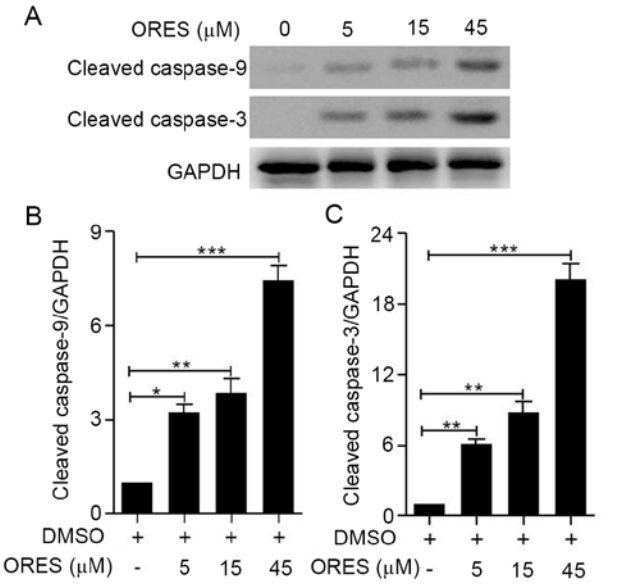

Figure 3. ORES enhances the expression of cleaved caspase-9 and cleaved caspase-3 in Saos-2 cells. Saos-2 cells were incubated with ORES at 0, 5, 15 and 45 μM for 24 h. The cells were then lysed in loading buffer. (A) Cleaved caspase-9 and cleaved caspase-3 were detected by western blotting. Semi-quantification of (B) cleaved caspase-9 and (C) cleaved caspase-3 was carried out using ImageJ software. The experiments were repeated three times and the results are shown as the mean ± SEM. *P<0.05, **P<0.01, ***P<0.001. ORES, oxyresveratrol.

ORES induces apoptosis and inhibits cell viability via STAT3 phosphorylation in Saos-2 cells. Given that STAT3 serves an important role in the proliferation and apoptosis of osteosarcoma cells (17), STAT3 activation in Saos-2 cells upon treatment with ORES was further examined. Compared with those of the untreated group, after treatment with ORES at 5, 15 and 45 μM for 24 h, the expression levels of P-STAT3 were significantly reduced in a concentration-dependent manner (Fig. 5A and B), whereas no significant differences were observed in the expression levels of T-STAT3 (Fig. 5A and C). OPN is regulated by STAT3 signaling, which is involved in osteosarcoma pathogenesis (21). Compared with those of the untreated group, treatment with ORES significantly decreased the expression levels of OPN (Fig. 5A and D). To determine whether ORES inhibits Saos-2 cell viability via a reduction in STAT3 activation, IL-6 was used to activate STAT3 signaling (36) in Saos-2 cells and reverse the effects of ORES. Upon treatment with 30 μM ORES for 24 h, the phosphorylation of STAT3 was induced by co-stimulation with 20 ng/ml IL-6 (Fig. 6A and B). After incubation with 20 ng/ml IL-6, the effects of ORES on the percentage of apoptotic cells (Fig. 6C and D) and cell viability (Fig. 6E) were reversed. These results indicated that ORES induces apoptosis and inhibits cell viability via partially reducing STAT3 signaling in Saos-2 cells.

Discussion

The results of the present study demonstrated that ORES effectively inhibited cell viability and induced apoptosis of Saos-2 cells. Upon treatment with ORES, the expression levels of cleaved caspase-9 and cleaved caspase-3 were significantly

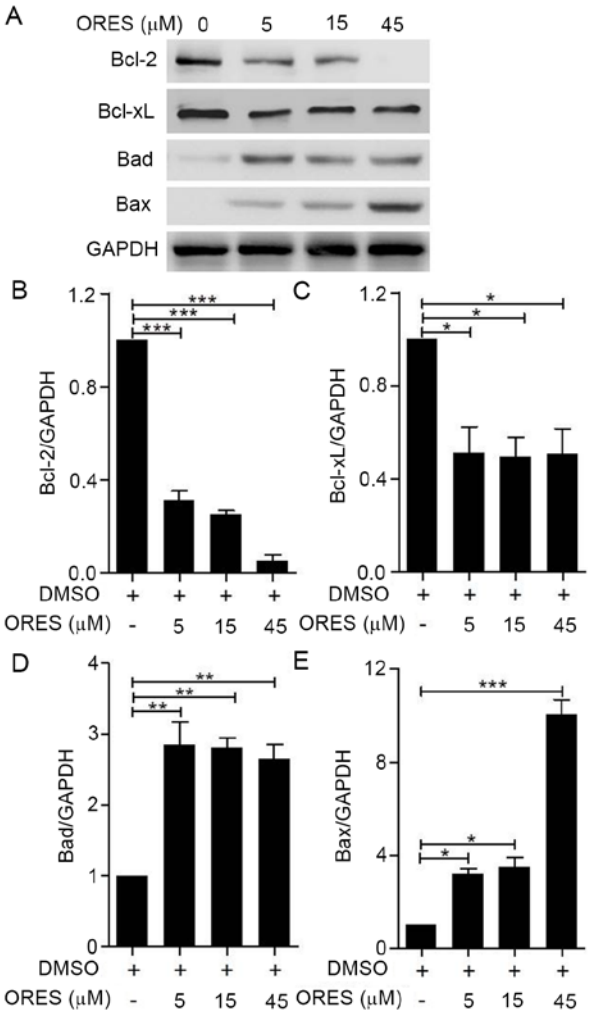

Figure 4. ORES modulates apoptotic signaling pathways in Saos-2 cells. Saos-2 cells were incubated with ORES at 0, 5, 15 and 45 μM for 24 h. (A) Apoptotic signal pathway-related proteins Bcl-2, Bcl-xL, Bad and Bax were detected by western blotting. GAPDH was measured as a loading control. The expression levels of (B) Bcl-2, (C) Bcl-xL, (D) Bad and (E) Bax were semi-quantified using ImageJ software. The experiments were repeated three times and the results are shown as the mean ± SEM. *P<0.05, **P<0.01, ***P<0.001. ORES, oxyresveratrol.

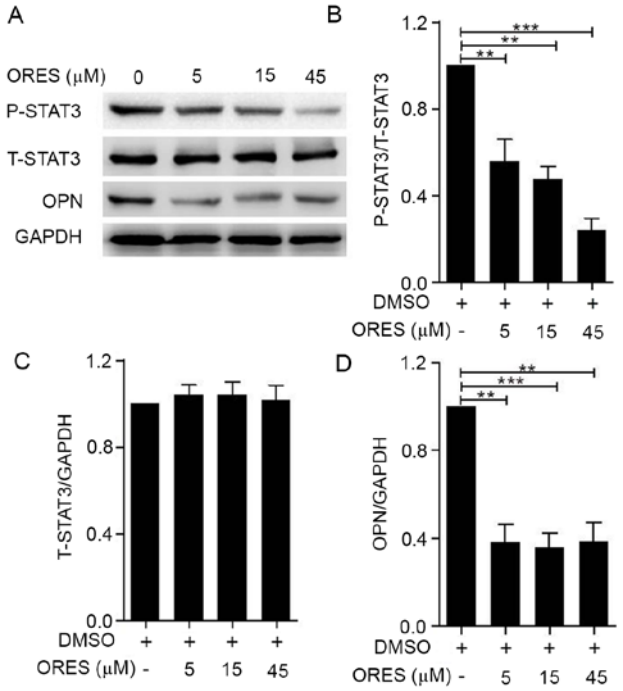

Figure 5. ORES attenuates the phosphorylation of STAT3 and the expression levels of OPN in Saos-2 cells. Saos-2 cells were incubated with ORES at 0, 5, 15 and 45 μM for 24 h. (A) Phosphorylation of STAT3 and the expression levels of T-STAT3, OPN and GAPDH were detected by western blotting. The ratio of (B) P-STAT3 to T-STAT3 and the expression levels of (C) T-STAT3 and (D) OPN were quantified by ImageJ software. The experiments were repeated three times and the results are shown as the mean ± SEM. **P<0.01, ***P<0.001. ORES, oxyresveratrol; OPN, osteopontin; P-STAT3, phosphorylated STAT3; T-STAT3, total STAT3.

increased. Additionally, the expression levels of anti-apoptotic proteins Bcl-2 and Bcl-xL were decreased, whereas the expression levels of the pro-apoptotic proteins Bad and Bax were upregulated. These results indicated that ORES has specific antitumor activity against Saos-2 cells.

ORES is a natural compound derived from *Morus alba* L., and its roles have been revealed in various disease models. In macrophages, ORES has been proven to suppress LPS-stimulated inflammatory responses by blocking the MAPK signaling pathway (26). In addition to its anti-inflammatory effects, ORES significantly inhibited the proliferation of hepatocellular carcinoma (HCC) cells (37), and head and neck squamous cell carcinoma cells (28). In both cases, the expression levels of vascular endothelial growth factor (VEGF) were inhibited by ORES treatment, which indicates that ORES may reduce micro-blood vessel density and micro-lymphatic vessel density in tumors. As VEGF expression is regulated directly by STAT3 in diverse human cancer cell lines (38), in addition to inhibition of cell viability, ORES may target STAT3-mediated VEGF expression in osteosarcoma. The inhibitory concentrations of ORES in various tumor cells were different. The IC_{50} value of ORES in T24 bladder cancer cells was 47.46 μM (39). In HCC cells, the IC_{50} values were nearly 80 μM (37). As for neuroblastoma cells, the IC_{50} values reached 140 μM, with little inhibitory effect against non-cancer cells, such as Rat-2, HEK293, NIH3T3 and human peripheral blood mononuclear cells (29). Therefore, Saos-2 cells were relatively sensitive to ORES with an IC_{50} of <15 μM. In view of the broad biological activities of ORES, especially its significant antitumor effects, further research should focus on both cancer cells and tumor-surrounding cells, including endothelial cells and immune cells.

It has been reported that multiple signaling pathways influence the process of osteosarcoma cell growth and anti-apoptosis, which can be interfered with using small molecule compounds (40-42). For instance, caffeine has been shown to induce apoptosis of osteosarcoma cells by inhibiting the AKT/mTOR/ribosomal protein S6 kinase, NF-κB and MAPK pathways (40). Glycogen synthase kinase 3 inhibitors have also been demonstrated to inhibit proliferation in osteosarcoma cell lines U2OS and MG-63 *in vitro* (41). Messerschmitt *et al* (42) reported that specific tyrosine kinase inhibitors, such as inhibitors of EGF-R, insulin-like growth factor 1 and Met, decreased motility and colony formation in human osteosarcoma cell lines. Signaling pathways, such as the hedgehog (43), Wnt (44) and PI3K/AKT signaling pathways (45), are all involved in osteosarcoma proliferation. Notably, recently

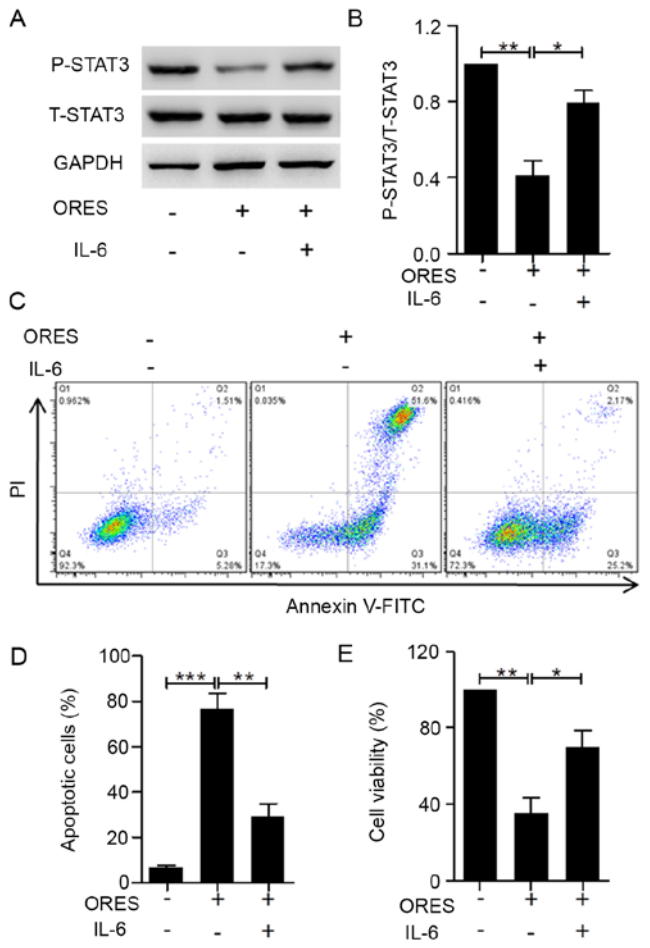

Figure 6. STAT3 activation rescues ORES-induced apoptosis and inhibits proliferation of Saos-2 cells. Saos-2 cells were incubated with 30 μM ORES or 30 μM ORES and 20 ng/ml IL-6 for 24 h. (A) P-STAT3 and T-STAT3 expression levels were detected via western blotting. (B) Ratio of P-STAT3 to T-STAT3 was semi-quantified with ImageJ software. (C) Apoptosis of Saos-2 cells was identified by staining with Annexin V-FITC/PI and detected using flow cytometry. (D) Percentage of apoptotic cells was quantified. (E) Cell viability was measured using the Cell Counting Kit-8 assay. The experiments were repeated three times and the results are shown as the mean ± SEM. *P<0.05, **P<0.01, ***P<0.001. ORES, oxyresveratrol; P-STAT3, phosphorylated STAT3; T-STAT3, total STAT3; PI, propidium iodide.

discovered types of cell death, such as receptor-interacting protein (RIP)1- and RIP3-dependent necroptosis, as well as Ca^{2+}/calmodulin-dependent protein kinase type II a activity-related autophagic degradation, have been considered as efficient anti-osteosarcoma strategies in recent research (46,47). Resveratrol, which is structurally similar to ORES, has been shown to induce the apoptosis of osteosarcoma cells via modulating the microRNA139-5p/NOTCH1 signaling pathway (48). Additionally, resveratrol can inhibit osteosarcoma MG-63 and MNNG/HOS cell proliferation and tumorigenesis via blocking janus kinase (JAK)2/STAT3 signaling (49). Consistent with this, in the present study, as a potent tyrosinase inhibitor, ORES inhibited the growth of osteosarcoma cells and promoted apoptosis by affecting the STAT3 signaling pathway, which indicated that STAT3 may be another drug target for ORES.

STAT3 has already been confirmed to serve a crucial role in selectively inducing and maintaining a carcinogenic inflammatory microenvironment in response to cytokine stimulation (17). The IL-6-JAK-STAT3 signaling axis contributes to the pathogenesis of myeloma cells by preventing apoptosis (50). By blocking the IL-6-OPN-STAT3 signaling pathway, the viability and tumorigenesis of osteosarcoma cells are inhibited (21). This is consistent with the findings of the present study, which demonstrated that compared with in the control group, the phosphorylation of STAT3 was attenuated by ORES treatment in Saos-2 cells. In addition, when P-STAT3 was partially activated by IL-6, the inhibition of cell viability and apoptosis promotion induced by ORES were also rescued. As a major cytokine in the tumor microenvironment, IL-6 protects cancer cells against apoptosis via multiple signaling pathways (51). The rescue of STAT3 phosphorylation may explain in part the reversal effect of ORES. Given that completely blocking STAT3 was demonstrated to be a risk factor causing other diseases, such as hyper-immunoglobulin E syndrome (52), inhibition of STAT3 should be under strict control. Local suppression of STAT3 for a limited period of time may convert inflammation in the tumor microenvironment from promoting tumor growth to inhibition without serious side effects (17). FDA-approved tyrosine kinase inhibitors, such as sorafenib (53) and sunitinib (54), are already in clinical use and can indirectly inhibit STAT3 signaling, resulting in tumor cell cycle arrest and the induction of apoptosis. The development of new STAT3 inhibitors may inhibit the viability and survival of multiple tumor cells.

In conclusion, the present study demonstrated the interaction between ORES and osteosarcoma. ORES induced apoptosis and inhibited cell viability by reducing STAT3 signaling in Saos-2 cells. More comprehensive studies of ORES may establish it as a promising agent for the future treatment of osteosarcoma.

Acknowledgements

Not applicable.

Funding

The present study was supported by the National Natural Science Foundation of China (grant no. 81971753), the Program for Medical Key Department of Shanghai (grant no. ZK2019C01), the Program for the Outstanding Clinical Discipline Project of Shanghai Pudong (grant no. PWYgy2018-09), the Key Disciplines Group Construction Project of Pudong Health Bureau of Shanghai (grant no. PWZxq2017-11), the Program for Outstanding Leader of Shanghai (grant no. 046), and the Talents Training Program of Pudong Hospital affiliated to Fudan University (grant no. PJ201903).

Availability of data and materials

All data generated or analyzed during this study are included in this published article.

Authors' contributions

BY designed the project and drafted the manuscript. TL and ZJ performed the experiments and drafted the manuscript.

DL, RA and XZ participated in data analysis and revised the manuscript. All authors read and approved the final manuscript.

Ethics approval and consent to participate

Not applicable.

Patient consent for publication

Not applicable.

Competing interests

The authors declare that they have no competing interests.

References

1. Mirabello L, Troisi RJ and Savage SA: International osteosarcoma incidence patterns in children and adolescents, middle ages and elderly persons. Int J Cancer 125: 229-234, 2009.
2. Heymann MF, Lezot F and Heyman D: The contribution of immune infiltrates and the local microenvironment in the pathogenesis of osteosarcoma. Cell Immunol 343: 103711, 2019.
3. Gorlick R, Janeway K, Lessnick S, Randall RL and Marina N; COG Bone Tumor Committee: Children's oncology group's 2013 blueprint for research: Bone tumors. Pediatr Blood Cancer 60: 1009-1015, 2013.
4. Mirabello L, Troisi RJ and Savage SA: Osteosarcoma incidence and survival rates from 1973 to 2004: Data from the surveillance, epidemiology, and end results program. Cancer 115: 1531-1543, 2009.
5. Lu KH, Lin RC, Yang JS, Yang WE, Reiter RJ and Yang SF: Molecular and cellular mechanisms of melatonin in osteosarcoma. Cells 8: 1618, 2019.
6. Zhang Y, Cai L, Li D, Lao YH, Liu D, Li M, Ding J and Chen X: Tumor microenvironment-responsive hyaluronate-calcium carbonate hybrid nanoparticle enables effective chemotherapy for primary and advanced osteosarcomas. Nano Res 11: 4806-4822, 2018.
7. Feng X, Xu W, Li Z, Song W, Ding J and Chen X: Immunomodulatory nanosystems. Adv Sci (Weinh) 6: 1900101, 2019.
8. Wang J, Li Z, Wang Z, Yu Y, Li D, Li B and Ding J: Nanomaterials for combinational radio-immuno oncotherapy. Adv Funct Mater Oct 7, 2020 (Epub ahead of print).
9. Lowe SW and Lin AW: Apoptosis in cancer. Carcinogenesis 21: 485-495, 2000.
10. Fulda S and Debatin KM: Extrinsic versus intrinsic apoptosis pathways in anticancer chemotherapy. Oncogene 25: 4798-4811, 2006.
11. Bhola PD and Letai A: Mitochondria-judges and executioners of cell death sentences. Mol Cell 61: 695-704, 2016.
12. Adams JM and Cory S: The Bcl-2 apoptotic switch in cancer development and therapy. Oncogene 26: 1324-1337, 2007.
13. Chen G, Wang F, Trachootham D and Huang P: Preferential killing of cancer cells with mitochondrial dysfunction by natural compounds. Mitochondrion 10: 614-625, 2010.
14. Hu Y, Yu K, Wang G, Zhang D, Shi C, Ding Y, Hong D, Zhang D, He H, Sun L, *et al*: Lanatoside C inhibits cell proliferation and induces apoptosis through attenuating Wnt/β-catenin/c-Myc signaling pathway in human gastric cancer cell. Biochem Pharmacol 150: 280-292, 2018.
15. Wang Z, Yu K, Hu Y, Su F, Gao Z, Hu T, Yang Y, Cao X and Qian F: Schisantherin A induces cell apoptosis through ROS/JNK signaling pathway in human gastric cancer cells. Biochem Pharmacol 173: 113673, 2020.
16. Ashkenazi A, Fairbrother WJ, Leverson JD and Souers AJ: From basic apoptosis discoveries to advanced selective BCL-2 family inhibitors. Nat Rev Drug Discov 16: 273-284, 2017.
17. Yu H, Pardoll D and Jove R: STATs in cancer inflammation and immunity: A leading role for STAT3. Nat Rev Cancer 9: 798-809, 2009.
18. Wang YC, Zheng LH, Ma BA, Zhou Y, Zhang MH, Zhang DZ and Fan QY: Clinical value of signal transducers and activators of transcription 3 (STAT3) gene expression in human osteosarcoma. Acta Histochem 113: 402-408, 2011.
19. Wang X, Goldstein D, Crowe PJ and Yang JL: Impact of STAT3 inhibition on survival of osteosarcoma cell lines. Anticancer Res 34: 6537-6545, 2014.
20. Goel S, Sahu S, Minz RW, Singh S, Suri D, Oh YM, Rawat A, Sehgal S and Saikia B: STAT3-mediated transcriptional regulation of osteopontin in STAT3 loss-of-function related hyper IgE syndrome. Front Immunol 9: 1080, 2018.
21. Zhang C, Ma K and Li WY: Cinobufagin suppresses the characteristics of osteosarcoma cancer cells by inhibiting the IL-6-OPN-STAT3 pathway. Drug Des Devel Ther 13: 4075-4090, 2019.
22. Kim YM, Yun J, Lee CK, Lee H, Min KR and Kim Y: Oxyresveratrol and hydroxystilbene compounds. Inhibitory effect on tyrosinase and mechanism of action. J Biol Chem 277: 16340-16344, 2002.
23. Ortiz-Ruiz CV, Ballesta de Los Santos M, Berna J, Fenoll J, Garcia-Ruiz PA, Tudela J and Garcia-Canovas F: Kinetic characterization of oxyresveratrol as a tyrosinase substrate. IUBMB Life 67: 828-836, 2015.
24. Heo JI, Kim JH, Lee JM, Kho YJ, Lim SS, Park JB, Kim J, Kim SC and Lee JY: FOXO3a Activation by oxyresveratrol of *Morus bombycis* koidzumi extract mediates antioxidant activity. Anim Cells Syst 20: 39-47, 2016.
25. Jia YN, Lu HP, Peng YL, Zhang BS, Gong XB, Su J, Zhou Y, Pan MH and Xu L: Oxyresveratrol prevents lipopolysaccharide/D-galactosamine-induced acute liver injury in mice. Int Immunopharmacol 56: 105-112, 2018.
26. Lee HS, Kim DH, Hong JE, Lee JY and Kim EJ: Oxyresveratrol suppresses lipopolysaccharide-induced inflammatory responses in murine macrophages. Hum Exp Toxicol 34: 808-818, 2015.
27. Wei J, Chen JR, Pais EMA, Wang TY, Miao L, Li L, Li LY, Qiu F, Hu LM, Gao XM and Fan GW: Oxyresveratrol is a phytoestrogen exerting anti-inflammatory effects through NF-κB and estrogen receptor signaling. Inflammation 40: 1285-1296, 2017.
28. Sintuyanon N, Phoolcharoen W, Pavasant P and Sooampon S: Resveratrol demonstrated higher antiproliferative and antiangiogenic efficacy compared with oxyresveratrol on head and neck squamous cell carcinoma cell lines. Natural Prod Commun 12: 1781-1784, 2017.
29. Rahman MA, Bishayee K, Sadra A and Huh SO: Oxyresveratrol activates parallel apoptotic and autophagic cell death pathways in neuroblastoma cells. Biochim Biophys Acta Gen Subj 1861: 23-36, 2017.
30. Matencio A, Dhakar NK, Bessone F, Musso G, Cavalli R, Dianzani C, García-Carmona F, López-Nicolás JM and Trotta F: Study of oxyresveratrol complexes with insoluble cyclodextrin based nanosponges: Developing a novel way to obtain their complexation constants and application in an anticancer study. Carbohydr Polym 231: 115763, 2020.
31. Lee JH, Baek SY, Jang EJ, Ku SK, Kim KM, Ki SH, Kim CE, Park KI, Kim SC and Kim YW: Oxyresveratrol ameliorates nonalcoholic fatty liver disease by regulating hepatic lipogenesis and fatty acid oxidation through liver kinase B1 and AMP-activated protein kinase. Chem Biol Interact 289: 68-74, 2018.
32. Tadtong S, Chatsumpun N, Sritularak B, Jongbunprasert V, Ploypradith P and Likhitwitayawuid K: Effects of oxyresveratrol and its derivatives on cultured P19-derived neurons. Trop J Pharm Res 15: 2619-2628, 2016.
33. Lee HJ, Feng JH, Sim SM, Lim SS, Lee JY and Suh HW: Effects of resveratrol and oxyresveratrol on hippocampal cell death induced by kainic acid. Anim Cells Syst (Seoul) 23: 246-252, 2019.
34. Duan C, Han J, Zhang C, Wu K and Lin Y: Inhibition of kidney cancer cell growth by Mulberroside-A is mediated via mitochondrial mediated apoptosis, inhibition of cell migration and invasion and targeting EGFR signalling pathway. J BUON 24: 296-300, 2019.
35. Li ZR, Ma T, Guo YJ, Hu B, Niu SH, Suo FZ, Du LN, You YH, Kang WT, Liu S, *et al*: Sanggenon O induced apoptosis of A549 cells is counterbalanced by protective autophagy. Bioorg Chem 87: 688-698, 2019.
36. Che Q, Xiao X, Liu M, Lu Y, Doug X and Liu S: IL-6 promotes endometrial cancer cells invasion and migration through signal transducers and activators of transcription 3 signaling pathway. Pathol Res Pract 215: 152392, 2019.
37. Liu Y, Ren W, Bai Y, Wan L, Sun X, Liu Y, Xiong W, Zhang YY and Zhou L: Oxyresveratrol prevents murine H22 hepatocellular carcinoma growth and lymph node metastasis via inhibiting tumor angiogenesis and lymphangiogenesis. J Nat Med 72: 481-492, 2018.

38. Niu G, Wright KL, Huang M, Song L, Haura E, Turkson J, Zhang S, Wang T, Sinibaldi D, Coppola D, *et al*: Constitutive Stat3 activity up-regulates VEGF expression and tumor angiogenesis. Oncogene 21: 2000-2008, 2002.
39. Yang Y, Zhang G, Li C, Wang S, Zhu M, Wang J, Yue H, Ma X, Zhen Y and Shu X: Metabolic profile and structure-activity relationship of resveratrol and its analogs in human bladder cancer cells. Cancer Manag Res 11: 4631-4642, 2019.
40. Miwa S, Sugimoto N, Yamamoto N, Shirai T, Nishida H, Hayashi K, Kimura H, Takeuchi A, Igarashi K, Yachie A and Tsuchiya H: Caffeine induces apoptosis of osteosarcoma cells by inhibiting AKT/mTOR/S6K, NF-κB and MAPK pathways. Anticancer Res 32: 3643-3649, 2012.
41. Lu K, Wang X, Chen Y, Liang D, Luo H, Long L, Hu Z and Bao J: Identification of two potential glycogen synthase kinase 3β inhibitors for the treatment of osteosarcoma. Acta Biochim Biophys Sin (Shanghai) 50: 456-464, 2018.
42. Messerschmitt PJ, Rettew AN, Brookover RE, Garcia RM, Getty PJ and Greenfield EM: Specific tyrosine kinase inhibitors regulate human osteosarcoma cells in vitro. Clin Orthop Relat Res 466: 2168-2175, 2008.
43. Kumar RM and Fuchs B: Hedgehog signaling inhibitors as anti-cancer agents in osteosarcoma. Cancers (Basel) 7: 784-794, 2015.
44. McQueen P, Ghaffar S, Guo Y, Rubin EM, Zi XL and Hoangn BH: The Wnt signaling pathway: Implications for therapy in osteosarcoma. Expert Rev Anticancer Ther 11: 1223-1232, 2011.
45. Qian H, Huang T, Chen Y, Li X, Gong W, Jiang G, Zhang W, Cheng S, Li X and Li P: X-linked inhibitor of apoptosis protein inhibitor Embelin induces apoptosis via PI3K/Akt pathway and inhibits invasion in osteosarcoma cells. J Cancer Res Ther 14 (Supplement): S648-S655, 2018.
46. Li S, Zhang T, Xu W, Ding J, Yin F, Xu J, Sun W, Wang H, Sun M, Cai Z and Hua Y: Sarcoma-targeting peptide-decorated polypeptide nanogel intracellularly delivers shikonin for upregulated osteosarcoma necroptosis and diminished pulmonary metastasis. Theranostics 8: 1361-1375, 2018.
47. Xu J, Wang H, Hu Y, Zhang YS, Wen L, Yin F, Wang Z, Zhang Y, Li S, Miao Y, *et al*: Inhibition of CaMKIIα activity enhances antitumor effect of fullerene C60 nanocrystals by suppression of autophagic degradation. Adv Sci (Weinh) 6: 1801233, 2019.
48. Xiao X, Zhang Y, Pan W and Chen F: MiR-139-mediated NOTCH1 regulation is crucial for the inhibition of osteosarcoma progression caused by resveratrol. Life Sci 242: 117215, 2020.
49. Peng L and Jiang D: Resveratrol eliminates cancer stem cells of osteosarcoma by STAT3 pathway inhibition. PLoS One 13: e0205918, 2018.
50. Catlett-Falcone R, Landowski TH, Oshiro MM, Turkson J, Levitzki A, Savino R, Ciliberto G, Moscinski L, Fernández-Luna JL, Nuñez G, *et al*: Constitutive activation of Stat3 signaling confers resistance to apoptosis in human U266 myeloma cells. Immunity 10: 105-115, 1999.
51. Kumari N, Dwarakanath BS, Das A and Bhatt AN: Role of interleukin-6 in cancer progression and therapeutic resistance. Tumour Biol 37: 11553-11572, 2016.
52. Minegishi Y, Saito M, Tsuchiya S, Tsuge I, Takada H, Hara T, Kawamura N, Ariga T, Pasic S, Stojkovic O, *et al*: Dominant-negative mutations in the DNA-binding domain of STAT3 cause hyper-IgE syndrome. Nature 448: 1058-1062, 2007.
53. Yang F, Van Meter TE, Buettner R, Hedvat M, Liang W, Kowolik CM, Mepani N, Mirosevich J, Nam S, Chen MY, *et al*: Sorafenib inhibits signal transducer and activator of transcription 3 signaling associated with growth arrest and apoptosis of medulloblastomas. Mol Cancer Ther 7: 3519-3526, 2008.
54. Xin H, Zhang C, Herrmann A, Du Y, Figlin R and Yu H: Sunitinib inhibition of Stat3 induces renal cell carcinoma tumor cell apoptosis and reduces immunosuppressive cells. Cancer Res 69: 2506-2513, 2009.